Title
Possible Global Magneto-Fluid Structure of the Stellar Convection Zone

Journal
Publications of the Astronomical Society of Japan, 58(3)

ISSN
0004-6264

Authors
Itoh, Sanae I
Itoh, Kimitaka
Diamond, Patrick H
et al.

Publication Date
2006-06-25

DOI
10.1093/pasj/58.3.605

Peer reviewed

Author's submitted version
Published as:
The Astronomical Society of Japan 58, 605, 2006
https://doi.org/10.1093/pasj/58.3.605

Possible Global Magneto-Fluid Structure of the Solar Convection Zone

S.-I. Itoh[1], K. Itoh[2], P. H. Diamond[3], A. Yoshizawa[2]

[1]Research Institute for Applied Mechanics, Kyushu University, Kasuga 816-8580, Japan
[2]National Institute for Fusion Science, Toki 509-5292, Japan
[3]Department of Physics, University of California San Diego, San Diego CA 92093-0319, U.S.A.

Abstract

Structures of the magnetic field and velocity in the sun are discussed based on the mean field MHD equations. A special case is presented, where the solution is constructed by the Beltrami solution in the convection zone with the symmetry in the azimuthal direction. Magnetic field lines form concentric toroidal magnetic surfaces. Relation of this toroidal magnetic structure with the polarity rule of the sunspots is discussed. The cross-helicity dynamo mechanism induces a mean flow of plasmas. The structure of this driven flow is also shown to constitute toroidal surfaces. Considering the symmetry, it is shown that the latitudinal component of this flow is pole-ward in the northern as well as southern hemispheres. This gives an insight into the role of magnetic field for the meridional flow in the sun.

1. Introduction

Structure of the sun, especially the magnetic and flow structure, has attracted attentions. The progress of the helioseismology has shown a new aspect of the flow such as the tachocline, periodic torsional oscillation and the meridional flow, and has provided challenges for the solar physics. [1]

The magnetic structure and flow structure in convection zone have been subject to intensive studies in relation with the dynamo problems. (See, e.g., reviews [2-8].) The effect of the magnetic field on the flow is reconsidered as is recently summarized [9], and requires further studies. Besides the conventional turbulent dynamo mechanisms like alpha- and beta dynamo (i. e., the turbulent helicity effect and turbulent resistivity), the gamma-dynamo (turbulent cross-helicity dynamo) has been predicted [10]. In this mechanism, the electromotive force is driven in proportion to the fluid vorticity. The counterpart of this process appears in the equation of the fluid dynamics. That is, the turbulence force, which is in proportion to the inhomogeneous mean magnetic field, appears when the turbulent cross-helicity does not vanish.

This mechanism is applied to the solar plasmas. One example is given in the problem of generation of toroidal and poloidal magnetic field in the sun and the reversal of magnetic field. The other example discusses the relationship between the solar magnetic activity (as is revealed as sun spots) and the torsional oscillation. In addition to the Lorenz force model [11], the gamma-dynamo mechanism has been discussed [12]. Not only the activity of solar rotation on the surface, but also their internal structure in the convection zone show the similar structure of oscillating component, although their entire picture is not observed at high precision. It was shown that, on top of the stationary velocity structure of the solar tachocline, the toroidal plasma flow can be induced by the solar magnetic field.

This article reports the possible magneto-fluid structures of the convection zone of the sun in the presence of strong gamma-dynamo process. Possible stationary structures are discussed, but dynamics are not treated. Based on the turbulent electromotive force, a toroidal structure of magnetic field is explained. Then the plasma flow driven by this magnetic field through the cross-helicity dynamo mechanism is discussed. It is shown that the meridional flow can be induced by the toroidal magnetic structures. When the magnetic field satisfies the polarity rule (i. e., the symmetry property across the equatorial plane), the meridional flow driven by the gamma-dynamo mechanism directs pole-ward both in the northern and southern hemispheres.

In §2, basic equations to start with are shown, together with the imposed boundary conditions. Assumptions are introduced. Then, the formal solutions of magnetic field and the flow structures are obtained in a spherical geometry. In §3, the solutions are shown and the structures of the magnetic field and flow velocity are illustrated. Implications of the solution are discussed. In the final section, summary and discussions are given.

2. Basic equations

One way to explain the meridional flow is based on the Eddington-Sweet mechanism [13] which is caused by the temperature gradient of the latitudinal direction. (Such a case is discussed in the Appendix A.) We in this article study a role of coupling between the magnetic field and flow. In order to study this mechanism, we assume, for the transparency of the argument, that the barochrinicity is ignored and the thermal wind balance holds. The basic equations we start with are the mean-field MHD equations in the following [14], i.e.,

$$\frac{\partial u_i}{\partial t} + \frac{\partial}{\partial x_j} u_i u_j = -\frac{\partial p}{\partial x_i} + 2\left(u \times \boldsymbol{\omega}_\mathrm{F}\right)_i + \left(\boldsymbol{J} \times \boldsymbol{B}\right)_i + \frac{\partial}{\partial x_j}\left(-R_{ij}\right) + \nu \nabla^2 u_i \ , \tag{1}$$

in the frame rotating with angular velocity $\boldsymbol{\omega}_\mathrm{F}$, and the induction equation

$$\frac{\partial \mathbf{B}}{\partial t} = \nabla \times \left(\mathbf{u} \times \mathbf{B} + \mathbf{E}_T\right) + \eta \nabla^2 \mathbf{B}. \tag{2}$$

where the turbulent electromotive force and Reynolds stress are given as

$$\mathbf{E}_T \equiv \langle \mathbf{u}' \times \mathbf{B}' \rangle = \alpha \mathbf{B} - \beta \mathbf{J} + \gamma \left(\boldsymbol{\omega} + 2\boldsymbol{\omega}_{\mathrm{F}} \right), \tag{3}$$

$$R_{ij} \equiv \left\langle u_i' u_j' - B_i' B_j' \right\rangle = -\frac{1}{3}\left\langle \mathbf{u}'^2 - \mathbf{B}'^2 \right\rangle \delta_{ij} + \nu_T \left(\frac{\partial u_j}{\partial x_i} + \frac{\partial u_i}{\partial x_j} \right) - \nu_M \left(\frac{\partial B_j}{\partial x_i} + \frac{\partial B_i}{\partial x_j} \right). \tag{4}$$

Here, Eq.(1) is the global flow equation in the presence of microscopic MHD turbulence, $\boldsymbol{u}$ is the relative velocity in the rotation frame, p is the pressure per unit mass with effects of microscopic pressure fluctuation included, $\boldsymbol{B}$ is the magnetic field, $\mathbf{J}\ (= \nabla \times \mathbf{B})$ is the electric current, ν is the kinematic viscosity, and η is the magnetic diffusivity. These equations are given in the Alfven unit, where the magnetic field is normalized to $\sqrt{\mu_0 \rho}$ and is measured in m/s (ρ is the mass density). Quantities with prime ($'$) indicate the fluctuating elements. Turbulent transport coefficients are defined as

$$\alpha = C_\alpha \left\langle - \boldsymbol{u}' \cdot \nabla \times \boldsymbol{u}' + \boldsymbol{B}' \cdot \nabla \times \boldsymbol{B}' \right\rangle \tau_c \ , \ \beta = C_\beta \left\langle \frac{1}{2}\boldsymbol{u}'^2 + \frac{1}{2}\boldsymbol{B}'^2 \right\rangle \tau_c \ ,$$
$$\gamma = C_\gamma \left\langle \boldsymbol{u}' \cdot \boldsymbol{B}' \right\rangle \tau_c \ , \ \nu_T = C_{\nu u}\beta, \ \nu_M = C_{\nu B}\gamma \ ,$$

where τ_c is the correlation time of turbulence, and C_α , C_β , C_γ , $C_{\nu u}$ and $C_{\nu B}$ are positive numerical coefficients, details of which are given in [7]. Equation (3) illustrates the conventional α -dynamo (helicity dynamo), β -dynamo (turbulent resistivity), and the γ -dynamo (cross-helicity dynamo). Note that the symbol γ indicates the cross-helicity dynamo in this article, and does not denote the anti-symmetric part of α which is used in, e.g., [2]. The gradient of the mass-weighted pressure appears in Eq.(1) as a total derivative ∇p . Mean field dynamical equations have been studied in rotating system (e.g., [15]), and this model of mean field equations is consistent with the line of thoughts in [15].

In order to obtain the possible solution with a global structure, we consider the case where the turbulent viscosity is large enough in comparison with the molecular viscosity, and the resistive diffusion of the magnetic field is neglected. For the transparency of the argument, the stationary solution $\partial \boldsymbol{B}/\partial t = 0$ for the case of constant dynamo coefficients of (α, β, γ) is considered. Under this circumstance, substitution of Eq. (3) into Eq. (2) gives the relation

$$\frac{\partial \mathbf{B}}{\partial t} = \nabla \times \left(\mathbf{u} \times \mathbf{B} + \alpha \mathbf{B} - \beta \mathbf{J} + \gamma \left(\boldsymbol{\omega} + 2\boldsymbol{\omega}_{\mathrm{F}} \right) \right). \tag{5}$$

We are interested in the case of $\boldsymbol{u} \,//\, \boldsymbol{B}$, and employ the approximation of dropping $\mathbf{u} \times \mathbf{B}$. The velocity fields are separated into two categories. The former is the flow velocity $\boldsymbol{u}_0$ which exists without the induction by the magnetic field. The other is the response of the flow velocity $\boldsymbol{u}$ owing to the appearance of the dynamo magnetic field. Properties of flows in the sun has been reviewed in [16]. We, in this article, are interested in and study the latter flow. The quasi-stationary sate of $\mathbf{B}$ may occur through the condition

$$\mathbf{J} = \frac{1}{\beta} \left(\alpha \mathbf{B} + \gamma \left(\boldsymbol{\omega} + 2\boldsymbol{\omega}_{\mathrm{F}} \right) \right). \tag{6}$$

We substitute Eq. (6) into Eq. (1). We take the curl of the resulting equation, and have the equation of the velocity which is driven by the magnetic field as

$$\frac{\partial \boldsymbol{\omega}}{\partial t} = \nabla \times \left(2\left(\boldsymbol{u} - \frac{\gamma}{\beta} \boldsymbol{B} \right) \times \boldsymbol{\omega}_{\mathrm{F}} + \nu_{\mathrm{T}} \nabla^2 \left(\boldsymbol{u} - \frac{\gamma}{\beta} \boldsymbol{B} \right) \right) . \tag{7}$$

The source of the torque $\nu_{\mathrm{T}} \nabla^2 (\gamma/\beta) \boldsymbol{B}$ in Eq.(7) is the counterpart of the γ -related term in the right-hand side (RHS) of Eq. (5). (Note that other type of solutions, with $\boldsymbol{u} \perp \boldsymbol{B}$ -components, also are able to exist. We focus here to the special solutions of $\boldsymbol{u} \,//\, \boldsymbol{B}$. The structure obtained here shows analytic insight to the problem as is discussed later in this article.) It has been well known that the turbulent transport coefficient α is quenched, in comparison with the evaluation based on the kinematic evaluation, by the generated mean magnetic field [6]. It is possible that the turbulent viscosity ν_{T} is also quenched by the generated mean magnetic field. In this article, we assume that the quenching rate of ν_T (for given generated mean magnetic field) is not stronger than the quenching of α .

Under these assumptions and conditions, the solutions which satisfy

$$\alpha \boldsymbol{B} - \beta \boldsymbol{J} + \gamma \left(\boldsymbol{\omega} + 2\, \boldsymbol{\omega}_F \right) = 0 \tag{8a}$$

and

$$\boldsymbol{u} = \frac{\gamma}{\beta} \boldsymbol{B} \tag{8b}$$

are searched for. From Eq.(8) and the relation $\boldsymbol{J} = \nabla \times \boldsymbol{B}$, we have

$$\nabla \times \boldsymbol{B} - \frac{\alpha}{\lambda_u \beta} \boldsymbol{B} = \frac{2\, \gamma}{\lambda_u \beta} \boldsymbol{\omega}_F \tag{9a}$$

where

$$\lambda_u \boldsymbol{B} = \boldsymbol{B} - \frac{\gamma}{\beta} \boldsymbol{u} = \left(1 - \left(\frac{\gamma}{\beta} \right)^2 \right) \boldsymbol{B} \tag{9b}$$

The homogeneous solution of Eq.(9) leads to the Beltrami solution of $\left(\boldsymbol{B}, \boldsymbol{J}, \boldsymbol{u}, \boldsymbol{\omega} \right)$,

$$\nabla \times \begin{pmatrix} \boldsymbol{B} \\ \boldsymbol{J} \\ \boldsymbol{u} \\ \boldsymbol{\omega} \end{pmatrix} = \frac{\alpha}{\lambda_u \beta} \begin{pmatrix} \boldsymbol{B} \\ \boldsymbol{J} \\ \boldsymbol{u} \\ \boldsymbol{\omega} \end{pmatrix} . \tag{10}$$

Inhomogeneous solutions are obtained accordingly, and the solution of our interest is shown after introducing the spherical coordinates.

In order to obtain the typical structures, we introduce the spherical coordinates $\left(r, \theta, \zeta \right)$, where $\theta = 0$ corresponds to the rotation axis, and the coordinates are shown in

Fig.1. The symmetry is imposed on the ζ -direction (toroidal direction, or latitudinal direction) $\partial/\partial\zeta = 0$.

In the beginning, we seek for the homogeneous solutions. Taking the rotation of Eq.(9a), we readily obtain

$$\nabla^2 \boldsymbol{B} + \left(\frac{\alpha}{\lambda_u \beta}\right)^2 \boldsymbol{B} = 0 \ . \tag{11}$$

The toroidal (longitudinal) component of the magnetic field B_ζ satisfies

$$\frac{1}{r^2}\frac{\partial}{\partial r}\left(r^2 \frac{\partial}{\partial r}\mathrm{B}_\zeta\right) + \frac{1}{\mathrm{r}^2 \sin\theta}\frac{\partial}{\partial\theta}\left(\sin\theta \frac{\partial}{\partial\theta}\mathrm{B}_\zeta\right) - \frac{1}{\mathrm{r}^2 \sin^2\theta}\mathrm{B}_\zeta + \left(\frac{\alpha}{\lambda_u \beta}\right)^2 \mathrm{B}_\zeta = 0 \ . \tag{12}$$

General solutions for B_ζ , and B_θ are formally written in terms of the n-th order spherical Bessell functions (j_n and n_n) and the associated Legendre function of $P_n^{(m)}$ as

$$\mathrm{B}_\zeta(\mathrm{r}, \theta) = \sum_n \left(a_n \mathrm{j}_n(y) + b_n \mathrm{n}_n(y)\right) P_n^{(1)}(\cos\theta) \tag{13a}$$

$$\mathrm{B}_\theta(\mathrm{r}, \theta) = -\frac{\alpha}{\lambda_u \beta}\sum_n \left(a_n\left(\frac{n\mathrm{j}_n(y)}{y^2} - \frac{\mathrm{j}_{n+1}(y)}{y}\right) + b_n\left(\frac{n\mathrm{n}_n(y)}{y^2} - \frac{\mathrm{n}_{n+1}(y)}{y}\right)\right) P_n^{(1)}(\cos\theta) \tag{13b}$$

$$\mathrm{B}_r(\mathrm{r}, \theta) = \sum_n \left(a_n \mathrm{j}_n(y) + b_n \mathrm{n}_n(y)\right) y^{-1}\left(\frac{2\cos\theta}{\sin\theta} P_n^{(1)}(\cos\theta) - P_n^{(2)}(\cos\theta)\right) \tag{13c}$$

where

$$y = \frac{\alpha}{\lambda_u \beta} r \ . \tag{13d}$$

The flow velocities, $\left(u_r, u_\theta, u_\zeta\right)$, are also given by using Eq.(8b) and Eq.(13). Thorough description of the representation in terms of spherical harmonics has been discussed in, e.g., [17].)

Inhomogeneous solution of $\boldsymbol{B}$, namely, the toroidal field $B_{\zeta 0}\hat{\zeta}$, comes from the rigid rotation and is given in a form of toroidal (longitudinal) magnetic field by Yoshizawa [18]. Taking into account of the screening effect λ_u here, a form is given

$$B_{\zeta 0} = \frac{2\gamma}{\lambda_u \beta}\, \omega_F\, r \sin\theta \, , \tag{14a}$$

and $u_{\zeta 0}$ is also obtained as

$$u_{\zeta 0} = \left(\gamma/\beta\right) B_{\zeta 0} \, . \tag{14b}$$

The total fields are given as $\boldsymbol{B}_{\rm tot} = \boldsymbol{B} + B_{\zeta 0}\hat{\zeta}$ and $\boldsymbol{u}_{\rm tot} = \boldsymbol{u} + u_{\zeta 0}\hat{\zeta}$, respectively.

3. Possible solutions for toroidal structure

Let us analyze possible magnetic and associated flow structures based on the solutions in §2. Here, plausible boundary conditions as well as the constraints are given, and the solutions are illustrated.

3.1 Magnetic torus

3.1.1 Toroidal structure

We here choose the lower order structure of poloidal harmonics n $(n \geq 1)$ which is even from the up-down symmetry. (That is, the form of toroidal structure is symmetric with respect to the equatorial plane. The up-down symmetry of the sign of the magnetic field is discussed later.) The boundary condition in radius is given at the lower and upper boundaries, $r = r_{in}$ and $r = r_{out}$. On these surfaces, the radial magnetic field vanishes. [Note that this condition is chosen for the case that the Taylor number is not very high.

In the limit of the large Taylor number, structures are expected to become homogeneous in the z-direction. If this is the case, the boundary condition is given in terms of the cylindrical radius r_c in Fig.1] (The solution which is regular at the center, $r = 0$, is discussed in the Appendix B.)

In terms of the variable y of Eq.(13d), the boundary conditions are given at $y_{in} = (\alpha / \lambda_u \beta)\, r_{in}$ and $y_{out} = (\alpha / \lambda_u \beta)\, r_{out}$. The condition $\mathrm{B}_\zeta(\mathrm{r}, \theta) = 0$ at $r = r_{in}$ and $r = r_{out}$ yields

$$\mathrm{j}_n(y_{in})\mathrm{n}_n(y_{out}) - \mathrm{j}_n(y_{out})\mathrm{n}_n(y_{in}) = 0 \ . \tag{15a}$$

and

$$\frac{y_{out}}{y_{in}} = \frac{r_{out}}{r_{in}} \ . \tag{15b}$$

This eigenvalue equation (15) provides a series of solutions, even if the poloidal mode number n is chosen. (For instance, $y_{out} = 3.46\pi,\ 6.73\pi,\ 10.04\pi \cdots$ for $n = 2$ and $r_{in}/r_{out} = 0.7$.) The eigenvalue is chosen here as the minimum eigenvalue which satisfies Eq.(15). The plausibility argument for this is given later in conjunction with the quenching of the dynamo coefficients [6]. (See the note [19].) Once the eigenvalue (y_{in}, y_{out}) is obtained, the magnetic field solution is given (putting $b_n = -\,\mathrm{j}_n(y_{in})\, \mathrm{n}_n^{-1}(y_{in})\, a_n$ into Eq.(13) as

$$\mathrm{B}_\zeta(\mathrm{r}, \theta) = a_n\left(\mathrm{j}_n(y) - \frac{j_n(y_{in})}{n_n(y_{in})}\mathrm{n}_n(y)\right) P_n^{(1)}(\cos\theta) + \frac{\gamma}{\lambda_u \beta}\,\omega_{\mathrm{F}}\, r \sin\theta \tag{16a}$$

$$\mathrm{B}_\theta(\mathrm{r}, \theta) = -\frac{\alpha}{\lambda_u \beta}\, a_n\left(\frac{n\mathrm{j}_n(y)}{y^2} - \frac{\mathrm{j}_{n+1}(y)}{y} - \frac{\mathrm{j}_n(y_{in})}{\mathrm{n}_n(y_{in})}\left(\frac{n\mathrm{n}_n(y)}{y^2} - \frac{\mathrm{n}_{n+1}(y)}{y}\right)\right) P_n^{(1)}(\cos\theta) \tag{16b}$$

$$\mathrm{B}_r(\mathrm{r}, \theta) = a_n \left(\frac{\mathrm{j}_n(y)}{y} - \frac{\mathrm{j}_n(y_{in})\mathrm{n}_n(y)}{y\, \mathrm{n}_n(y_{in})} \right) \left(\frac{2 \cos \theta}{\sin \theta} P_n^{(1)}(\cos \theta) - P_n^{(2)}(\cos \theta) \right)$$

(16c)

Now the coefficient a_n represents the magnitude of the magnetic field of the homogeneous solution.

The result Eq.(16) shows that the magnetic field lines constitute concentric toroidal surfaces. The radial and poloidal magnetic field is expressed as

$$\begin{pmatrix} B_r \\ B_\theta \end{pmatrix} = \begin{pmatrix} \frac{1}{r^2 \sin \theta} \frac{\partial}{\partial \theta} \psi \\ -\frac{1}{r \sin \theta} \frac{\partial}{\partial r} \psi \end{pmatrix} \quad (17)$$

where $\psi = r \sin \theta B_{\zeta,\mathrm{h}}$ and $B_{\zeta,\mathrm{h}}$ is the longitudinal component of the homogeneous solution of the magnetic field. The radial and poloidal components of magnetic surface satisfy the relation

$$\left(B_r, B_\theta\right) \cdot \nabla_\perp \psi = 0 \ , \quad (18)$$

where $\nabla_\perp$ represents the derivative in radial and poloidal directions. Thus, ψ is the stream function (flux function) of the magnetic field. The contour of ψ represents the cross-section of the toroidal magnetic surface. The cross-sections of the toroidal magnetic surfaces are shown in Fig.2. The lowest order number $n = 2$ represents the solution (shown in Fig.(2a), in which the toroidal structure extends from the equator to the pole, and the one magnetic axis exists in both of the northern and southern hemispheres, respectively. The case of $n = 4$ stands for the case that a pair of tori is sustained in both the northern and southern hemispheres (fig.2b). Two magnetic axes appear in both the hemispheres. In this case,the eigenvalue y_{out} is given as, $y_{out} = 3.73\pi, 6.88\pi, 10.14\pi \cdots$ for $r_{in}/r_{out} = 0.7$.

3.1.2 Magnetic field in lower-latitude region

We here discuss the polarity of the magnetic field. Noting the fact that the turbulent resistivity β is a scalar quantity but the turbulent helicity α and turbulent cross-helicity γ are pseudo-scalar, the ratios α/β and γ/β change the sign under the mirror transformation. Thus, we take that α/β and γ/β have the property of anti-symmetry across the equatorial plane. Equation (16a) shows that B_ζ change sign between the upper and lower hemisphere. (So is the radial component of the magnetic field.) The poloidal magnetic field (magnetic field component in the longitudinal direction) has the same sign across the equatorial plane. Figure 3 illustrates the polarity of the magnetic field on the magnetic surface. In the case of Fig. 3, the rotational transform of the magnetic field is chosen to be right-handed in the northern-hemisphere. Then, it is left-handed in the southern-hemisphere. The sign of the toroidal magnetic field is opposite, but the sign of the latitudinal magnetic field is common.

This result of the sign of the rotational transform is related to the polarity rule of the sunspot. The observations of the sunspots have shown that (i) the sign of the (toroidal) magnetic field is opposite between the northern and southern hemisphere. (ii) In addition to it, the latitudinal location of a pair of sunspots shows an inclination with respect to the latitude. That is, as is shown in Fig.4, the eastern sunspot is at the lower latitude (i.e., closer to the equatorial plane) compared to the western sunspot. (iii) This property also holds for the southern hemisphere. (iv) When a magnetic flux tube deviates from the toroidal magnetic surface (owing to certain instabilities, which are not specified here), the flux tube retains the memory of the rotational transform of the magnetic surface. Thus, the magnetic rotational transform in the Fig.3 naturally induces the latitudinal inclination of the pair of sunspots on the solar surface. The sign of the magnetic field in Fig.3 corresponds to the one in the right figure of Fig.4. If the magnetic field changes the sign in Fig.3, then the resultant sunspots are inclined as the left figure of Fig.4.

Before closing this subsection, we note the possible quenching effect of dynamo coefficients owing to the induced magnetic field. The magnitude of the magnetic field is simultaneously determined from the global structure. Let us consider the case that the large values are given for ratios α/β and γ/β in the kinematic theory of dynamo. That is, from Eq.(15a), a large number of radial nodes are allowed in between r_{in} and r_{out} for these values. As the generated magnetic field increases, the dynamo coefficient α is known to be quenched

$$\alpha = \frac{\alpha_0}{1 + R_M B^2 V^{-2}} , \qquad (19)$$

where α_0 is the estimate in the kinematic model, R_M is the magnetic Reynolds number and V^2 is a characteristic mean square velocity [6]. The reduction of α indicates that the eigenvalue $\left(y_{in}, y_{out}\right)$ takes the minimum value when the growth of the magnetic field is saturated. The eigenvalue $\left(y_{in}, y_{out}\right)$ determines the magnitude of the magnetic field.

The coefficient β is quenched slower than α [6, 20]. Therefore, the ratio of mean dynamo coefficients α / β becomes smaller when the magnitude of the mean magnetic field increases. As is shown in Eq.(13), the scale length in the real space is in proportion to β/α, the reduction of α/β means that the scale of the generated mean field becomes larger as the magnetic field becomes stronger. Accepting this consideration, we conclude that the radial scale of the toroidal structure becomes larger as the magnetic field becomes stronger. Therefore, the requirement, that the minimum of y_{in} is selected from Eq.(15), determines the magnitude of the magnetic field.

It is not yet concluded whether the coefficient ν_T and γ are quenched slower than α. The possibility of the quenching of ν_T is investigated, suggesting a slower quench than α. This issue will be discussed in a separate article [21].

3.1.3 Magnetic field in higher-latitude region

Observation of the magnetic field has shown that the magnetic field has different property in the higher latitude region. The projection of the poloidal (latitudinal) and toroidal (longitudinal) magnetic field on the surface is illustrated in Fig.5(a). This indicates that the magnetic field in the higher-latitudinal region is attributed to the second torus which has an opposite helicity in comparison with the fundamental torus in the lower latitudinal region. For instance, the toroidal magnetic field in the lower-latitudinal region of the upper hemisphere is right-handed for the case of Fig.3. (The helix of magnetic field line is right-handed, i.e., B_ζ is in the same direction as $\nabla \times \left(B_r \hat{r} + B_\theta \hat{\theta} \right)$.) The toroidal magnetic structure in the higher-latitudinal region is left-handed.

A pair of toroidal magnetic structure can be imbedded in a hemisphere as is illustrated in Fig.2(b). The change of helicity (i.e., right-handed in the lower-latitude torus and left-handed for the higher-latitude torus) occurs when the sign of the coefficient α is different. That is, α is positive in the lower-latitudinal region and is negative in the higher-latitudinal region. The difference of the sign of α is plausible owing to the geometrical consideration. The temperature gradient is perpendicular to the rotation axis in the lower-latitudinal region, and is parallel to the rotation axis in the higher latitudinal region. This leads to the difference in the turbulent convection as is discussed in [22]. The dependence of the coefficient α on the poloidal angle has also been discussed in literature, e.g., [23, 24]. Figure 5(b) indicates the pair of torus and direction of magnetic field in the upper hemisphere corresponding to the case of Fig.3. The magnetic field in the southern hemisphere has a parity relation in comparison with the northern hemisphere. The right (left)-handed torus is transformed into the left (right)-handed torus, respectively as is shown in Fig.6(a). When the direction of the magnetic field is changed (with the period of 22 years), the structure of magnetic field is shown in Fig.6(b).

3.2 Induced flow with toroidal structure

Equation (8b), $\boldsymbol{u} = \left(\gamma/\beta\right) \boldsymbol{B}$, shows that the induced flow, which is driven by gamma-dynamo effect, has the same pattern as the toroidal magnetic field. The stream function of the flow constitutes the concentric toroidal surfaces.

The flow velocity, which is induced by the gamma-dynamo effect, is parallel to the magnetic field line. However, the direction of the flow is different from the magnetic field as is illustrated in Fig.6. The symmetry property of the magnetic field reflects the symmetry of the flow pattern. First, the relation of a pair of torus in the northern hemisphere is considered. In the main torus (lower-latitude torus), γ is chosen positive. In the second torus, the sign of α is reversed. In addition, the direction of the magnetic field is reversed, compared to the main torus. Therefore the coefficient γ recovers the positive sign. Thus the coefficient γ remains positive in the northern hemisphere. This leads to the conclusion that the flow that is driven by the cross-helicity dynamo has the same direction as the magnetic field in the northern hemisphere when the magnetic field takes the sign of Fig.6(a). That is, the poloidal flow (latitudinal flow) velocity is towards the pole, but the toroidal flow (longitudinal flow) velocity changes sign between the lower-latitude and higher latitude regions. The cross-helicity dynamo process drive a toroidal flow. Therefore, the meridional flow closes itself on a torus. The poloidal flow is connected to the radial flow. The other property of the flow is that direction of the radial flow changes near the latitude where the toroidal flow changes its sign.

Next, the flow velocity in the southern hemisphere is considered. According to the parity consideration, the coefficient γ has an opposite sign in the southern hemisphere. The flow velocity is indicated in Fig.7(a). The toroidal flow is symmetric across the equatorial plane, but the latitudinal flow is anti-symmetric. That is, the poloidal flow (latitudinal flow) directs to the north pole in the northern hemisphere, and to the south pole in the southern hemisphere. The meridional flows are pole-ward in both hemispheres. This solution naturally reveals the meridional flow. The direction of the magnetic field changes associated with the solar magnetic cycle.

The case, where the sign of the magnetic field is changes, is illustrated in Fig.7(b). Owing to the change of the sign of the cross-helicity, the direction of the induced flow with respect to the magnetic field is reversed. As a result of this change, the flow velocity keeps the same direction. In both phases of the positive and negative magnetic field, the latitudinal component of the induced flow is pole-wards in the northern and southern hemispheres.

It is interesting to note that the plasma current $\boldsymbol{J}$ and the flow vorticity $\boldsymbol{\omega}$ are also parallel to the magnetic field, and the proportionality coefficients between them are $\alpha/\beta\lambda_u$ and α/β, respectively:

$$\boldsymbol{u} = \frac{\gamma}{\beta}\boldsymbol{B} \tag{22a}$$

$$\boldsymbol{J} = \lambda_J \boldsymbol{B} \qquad \lambda_J = \alpha/\beta\lambda_u \tag{22b}$$

$$\boldsymbol{\omega} = \lambda_\omega \boldsymbol{B} \qquad \lambda_\omega = \lambda_u \lambda_J = \alpha/\beta \tag{22c}$$

The whole structures of $\boldsymbol{B}, \boldsymbol{J}, \boldsymbol{u}, \boldsymbol{\omega}$ are simultaneously determined from this particular mechanism. And the strengths are determined by the balance between α, β, and γ.

4. Summary

In this article, the toroidal structure of the magnetic field and velocity in the sun was discussed in the case that the cross-helicity dynamo (gamma-dynamo) process is present. The mean field dynamo equations are solved in the convection zone. A special case is presented, where the solution is constructed by the Beltrami solution in the spherical coordinates with the symmetry in the longitudinal direction. Magnetic field lines were shown to form toroidal magnetic surfaces. Multiple toroidal magnetic surfaces, which are concentric, constitute a torus. Solution with two magnetic axes in the northern hemisphere (and in the solution hemisphere as well) was presented. The cross-helicity dynamo mechanism induces a mean flow of plasmas. The structure of this driven flow was also analyzed. The flow is parallel to the magnetic field line, and constitute toroidal surfaces. Considering the parity with respect to the equatorial plane, it was shown that the latitudinal component of the flow, which is driven by the cross-helicity dynamo, is pole-ward in the northern as well as southern hemispheres. This gives one possible explanation for the meridional flow in the sun. The toroidal flow (longitudinal flow), which is driven by the cross-helicity dynamo changes its sign between the lower latitudinal region and the higher-latitudinal region. The sign of the torsional oscillation differs between the lower and higher latitudinal regions: This difference may be attributed to the dependence of toroidal flow velocity on the latitude. The other property of the predicted flow is that direction of the radial flow changes near the latitude where the toroidal flow changes its sign. This might be able to examine in a near future.

The coupling between the magnetic field and flow has been discussed. In the vorticity equation, the rate of vorticity change has the term like $\nabla \times \nu_T \nabla^2 \left(\boldsymbol{u} - \gamma \boldsymbol{B}/\beta \right)$. One way to reduce this term is to quench the coefficient ν_T by the mean magnetic field. This is the Ω -quenching mechanism [25]. In this article, the elimination of the difference $\boldsymbol{u} - \gamma \boldsymbol{B}/\beta$ was studied in the context of the cross-helicity dynamo mechanisms. Therefore, these two mechanisms are not mutually exclusive.

This way of thinking provides additional insights into the solar physics. The relation with the polarity rule of the sunspot is discussed. In addition, the toroidal magnetic structure occupies a large portion of the plasma, the toroidal surfaces are in the equilibrium under the gravity. [If only a thin tube is magnetized, this tube may be subject to buoyancy motion and will be carried to the surface where the dynamo effect may be weak.] The stability of the established toroidal magnetic field structure is an important issue for future studies. For instance, a small resistivity can lead to the deviation of the magnetic field from the Beltrami solution. The deviation can cause instabilities, which then tend to restore the Taylor state [26]. The occurrence of small-scale symmetry-breaking perturbation at the edge of the torus has been observed on laboratory plasmas, a characteristic example of which was known as edge localized modes (ELMs) [27]. Future study of such MHD instabilities of the possible solar toroidal magnetic structure will enrich the understanding of the origin of sunspots. There are other solutions of the higher order n -th poloidal eigenmode structures. Higher n-components are included in the solution if the realistic boundary condition in the sun is fulfilled. However, in this paper we focus upon indicating a prototypical solution which can explain the flows towards the Arctic and Antarctic poles from the equator. More realistic solutions with precise boundary conditions are left for future work.

In brief, the essence of the argument presented here is that turbulence cross-helicity ($\langle \tilde{\mathbf{v}} \cdot \tilde{\boldsymbol{B}} \rangle$, which appears in γ) and mean potential vorticity $(\boldsymbol{\omega} + 2\boldsymbol{\omega}_F)$ may conspire to produce large scale magneto-fluid Beltrami structures (i.e., field-aligned flows) in stellar convection zones. While such structures are of possible relevance to the sun - as we discuss - they are of much greater potential interest in the context of young, rapidly rotating stars (YRRS), which have rotation periods of (at most) 1-2 days. YRRS exhibit several features which appear consistent with the sense of the discussion presented above. Convective YRRS exhibit both fast rotation and heightened magnetic activity, the latter increasing with rotation rate [28]. YRRS exhibit 'star spot' photospheric filling factors f as high as 30-50%, in dramatic contrast to the case of the sun ($f < 1\%$) [29]. YRRS also seem to be slightly larger than expected, according to standard stellar structure theory, and to exhibit concomitantly higher photospheric temperatures [30]. Thus, the internal magnetic field of YRRS may be strong enough to directly impact the spatiotemporal structure of their convective heat transport process. In addition, star spots are of general utility as photospheric flow 'marker particles', and the large spot filling factor should facilitate improved spatial resolution. It may thus be possible to map photospheric meridional flows in YRRS in the near future. Existing observations indicate that spots migrate toward the polar regions, again in contrast to the sun. In summary, then, YRRS combine large potential vorticity, convective turbulence, enhanced magnetic activity, and non-trivial meridional flow structure, all of which are linked by the theory presented in this paper. It seems quite reasonable, then, to speculate that such YRRS are prime candidates for manifesting the global magneto-fluid structures discussed in this paper. We will explore this speculation in future research.

ACKNOWLEDGEMENTS

Authors acknowledge discussions with Prof. H. Shibahashi, Dr. M. Yagi, Dr. N. Yokoi. They are grateful to Prof. F. Spineanu, Prof. M. Vlad and Dr. N. Kasuya for providing data of spherical functions. This work is partly supported by the Grant-in-Aid for Specially-Promoted Research of MEXT (16002005), by the collaboration programs of NIFS and of the Research Institute for Applied Mechanics of Kyushu University, by Asada Science Foundation, and by the U.S. DOE under Grant No. FG02-04ER54738. Main part of this work has been performed when one of the authors (AY) was the visiting professor at NIFS. One of the authors (PHD) acknowledges the hospitality of Kyushu University.

Appendix A: Hydrodynamic picture for meridional flows

The cause of the meridional flow has been considered, within a framework of the hydrodynamics, to be that the rotation frequency ω_F depends on (r, θ), $\omega_F(r, \theta)$, not $\omega_F(r_c)$. (Here r_c refers to the cylindrical radius, and (r_c, ζ, z) constitute the cylindrical coordinates, see Fig.1) Alternatively put, $\partial\omega_F / \partial z \neq 0$, so that the sun is not in a Taylor-Proudman state. As a result, the equilibrium condition from Eq.(7) is rewritten (neglecting gamma-dynamo effects) as

$$\frac{\partial \boldsymbol{\omega}}{\partial t} = \nabla \times \left(-\frac{\nabla P}{\rho} + 2\boldsymbol{u} \times \boldsymbol{\omega}_F + \nu_T \nabla^2 \boldsymbol{u} \right) \tag{A1}$$

where ρ : mass density , P : total pressure.

Further simplification is used as

$$\frac{\nabla \rho}{\rho} = -\frac{\nabla\, \delta T}{T} \tag{A2}$$

where δT denotes the temperature variation away from adiabatic relation. [In case of perfect adiabatic stratification, $\nabla\rho \times \nabla P = 0$ and $\nabla\rho \times \nabla T = 0$ hold.] When the hydrostatic balance in the radial direction, i.e., $\nabla P = \rho \boldsymbol{g}$, is satisfied ($\boldsymbol{g}$ is the gravitational acceleration, $\boldsymbol{g} = g\hat{r}$), the equation

$$-\frac{g}{rT}\frac{\partial\,\delta T}{\partial\theta}+r_c\frac{\partial\omega_F^2}{\partial z}-\frac{\partial}{\partial r}\left(\nu_T\nabla^2 u_\theta\right)=0 \tag{A3}$$

gives the balance relation for the poloidal flow.

Note that the relation

$$\frac{g}{rT}\frac{\partial\,\delta T}{\partial\theta}=r_c\frac{\partial\omega_F^2}{\partial z} \tag{A4}$$

has been known as the *thermal wind balance*. According to the hydrodynamics, the poloidal flow (meridional flow) is induced if the thermal wind balance is violated. In the sun, the rotation frequency is observed that Ω is larger at the equator than at high latitudes. So that

$$\frac{\partial\omega_F^2}{\partial z}<0 \tag{A5}$$

holds. The first term, $\frac{\partial\,\delta T}{\partial\theta}$ term, acts in opposite direction if

$$\frac{g}{rT}\frac{\partial\,\delta T}{\partial\theta}<0 \tag{A6}$$

i.e., the pole must be warmer and the equator cooler. [9, 13]

The discussion in the main text corresponds to the case of perfect adiabatic stratification, and the flow is driven by the gamma-dynamo process.

Appendix B: Solution which is regular at the center.

The main interest of this article is the study of toroidal structure in a shelluar domain such as convective zone. Recently, a proposal of the magnetic field in the central core of the sun has been given [31]. The domain where the magnetic field is generated is considered to include the center. Then toroidal structure, if it exists, is singular at the center. In such a case, the toroidal solution is given as

$$B_\zeta(r, \theta) = a_1 j_1(y) P_1^{(1)}(\cos\theta) + \cdots \tag{B1a}$$

$$B_\theta(r, \theta) = -\frac{\alpha}{\lambda_u \beta} a_1 \left(\frac{j_1(y)}{y^2} - \frac{j_2(y)}{y} \right) P_1^{(1)}(\cos\theta) + \cdots \tag{B1b}$$

$$B_r(r, \theta) = a_1 \frac{j_1(y)}{y} \left(\frac{2\cos\theta}{\sin\theta} P_1^{(1)}(\cos\theta) - P_1^{(2)}(\cos\theta) \right) + \cdots \tag{B1c}$$

where $+ \cdots$ indicates the higher harmonics. The eigenvalue condition is given at a radius where the radial magnetic field vanishes.

This solution has a dipole component as in [31], but has a topology of a torus. It is force free, so that the global magnetic energy which is associated with the mean magnetic field takes a (local) minimum. Therefore it is more stable in comparison with the solution with a pure dipole magnetic field.

References

[1] See, e. g., for introductory monograph, Lang, K. R. 2001, The Cambridge Encyclopedia of the Sun (Cambridge: Cambridge University Press)

[2] Moffat H K, Magnetic field generation in electrically conduncting fluids (Cambridge University Press, Cambridge 1978)

[3] Krause F and Raedler K-H 1980, Mean Field Electrodynamics and Dynamo Theory (Pregamon Press 1980).

[4] Priest, E. R. 1982, Solar Magnetohydrodynamics (Dordrecht: Reidel)

[5] Parker, E. N. 1993, ApJ, **408**, 707

[6] Diamond, P. H., D. W. Hughes and E.-J. Kim: "Self-consistent mean field electrodynamics in two and three dimensions" in *The Fluid Mechanics of Astrophysics and Geophysics* eds. A. M. Soward, C. A. Jones, D. W. Hughes and N. O. Weiss, (CRC Press, London, 2004) Vol 12, 145

[7] Yoshizawa, A, Itoh, S. -I., Itoh, K., & Yokoi, N. 2004, Plasma Phys. Contr. Fusion, **46**, R25

[8] Shibahashi, H. 2002, J. Plasma Fusion Res., **78** 497

[9] H. Shibahashi: "Solar cycle variations of the internal structure and dynamics", in Proceedings IAU Symposium No. 223, 2004 (A.V. Stepanov, E.E. Benevolenskaya & A.G. Kosovichev, eds, 2004 International Astronomical Union)

[10] Yoshizawa, A. 1990, Phys. Fluids, B **2**, 1589

[11] Yoshimura, H. 1981 *Ap.J.* **247**, 1102–1112.

[12] Itoh S-I, et al. 2005 Astrophys. J. **618** 1044

[13] Sweet P A, 1950 M.N.R.A.S. **110** 548

[14] Yoshizawa, A., Itoh, S. -I., & Itoh, K. 2003, Plasma and Fluid Turbulence: Theory and Modelling (Bristol: Institute of Physics)

[15] Rüdiger R and Kitchatinov L L 1990 A&A **236** 503

[16] Thompson M J, Christensen-Dalsgaard J, Miesch M S, Toomre J 2003 Annu. Rev. Astrophys. **41** 599

[17] Yoshimura, H. 1972 Ap. J. **178**, 863

[18] Yoshizawa, A., Kato, H., & Yokoi, N. 2000, ApJ, **537**, 1039

[19] This is also related to the consideration of minimum principle. Under the circumstance of the fully developed MHD turbulence, the final state is conjectured as the minimum energy state for given helicity (J. B. Taylor state). (See: J. B. Taylor: Rev. Modern Phys. **58** (1986) 741.) If this is so, the radial node numbers tend to decrease. At this moment, it is not clear whether the final state is completely free from other constraints. For instance, if the Taylor number is high, then the constraints of the Taylor-Proudman theorem may prohibit the access to the J. B. Taylor state. Thus, we do not require the minimum principle of magnetic energy for given magnetic helicity, but accept the smallest eigenvalue from Eq.(15).

[20] Gruzinov A V and Diamond P H 1994 *Phys. Rev. Lett.* **72** 1651

[21] Diamonf PH, Itoh SI and Itoh K, 2005 "Zeldovich theorem for cross-helicity and momentum transport in 2D MHD", paper in preparation

[22] F. H. Busse: Chaos **4** 123 (1994).

[23] Rüdiger R and Brandenbrug A 1995 A&A **296** 557

[24] Covass E, Tavakol R, Moss D 2001 A&A **371** 718

[25] Kitchatinov L L, Rüdiger R and Kueker M 1994 A&A **292** 125

[26] J. B. Taylor: Rev. Modern Phys. **58** (1986) 741

[27] S.-I. Itoh, K. Itoh, H. Zushi, A. Fukuyama.: Plasma Phys. Contr. Fusion **40** (1998) 879

[28] Donati J-F, et al. 2003 M. N. R. A. S. **345** 1145

[29] O'Neal D, Neff J E, Saar S H 1998 ApJ **507** 919

[30] Barnes J R, et al. 2004 M. N. R. A. S. **352** 589

[31] D. O. Gough, M. E. McIntyre *Nature* **394** (1998) 755

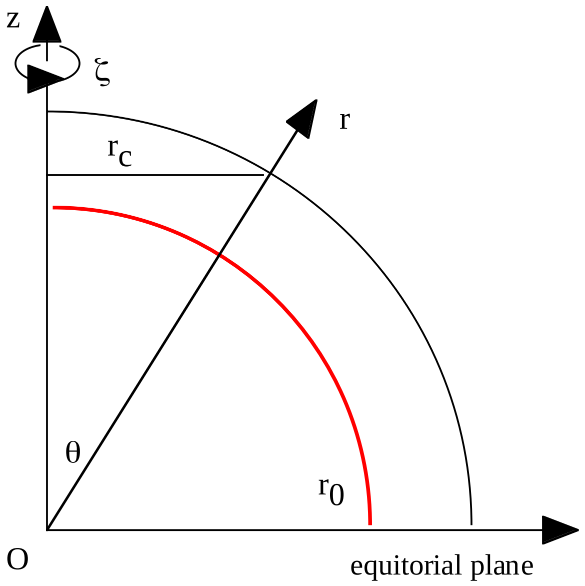

Fig.1 Spherical coordinates (r, θ, ζ) .

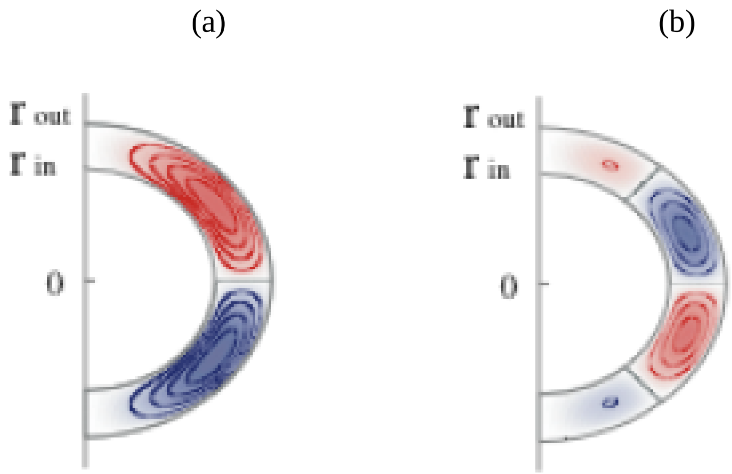

Fig.2 Cross-sections of the toroidal magnetic structure in the convective zone. The case of $n = 2$ (a) and $n = 4$ (b).

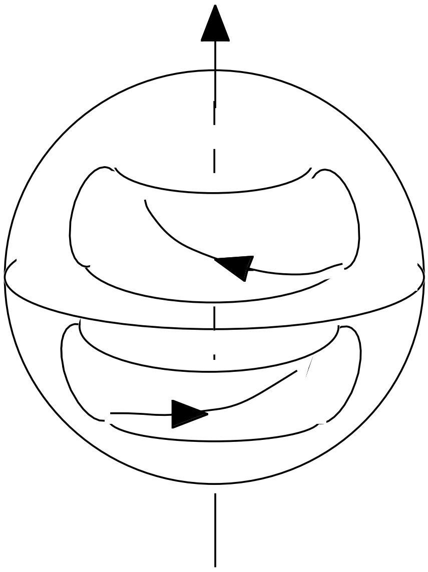

Fig.3 Schematic view of toroidal flux surfaces: one in the northern hemisphere and the other in the southern hemisphere.

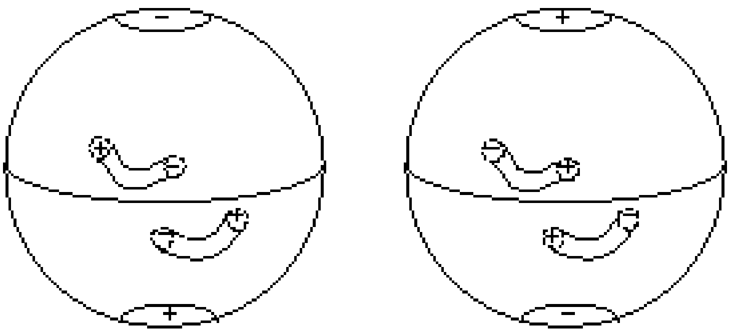

Fig.4 Polarity rule of the sunspot. With the period of 22 years, the state like left and that like right appears periodically. (From [12])

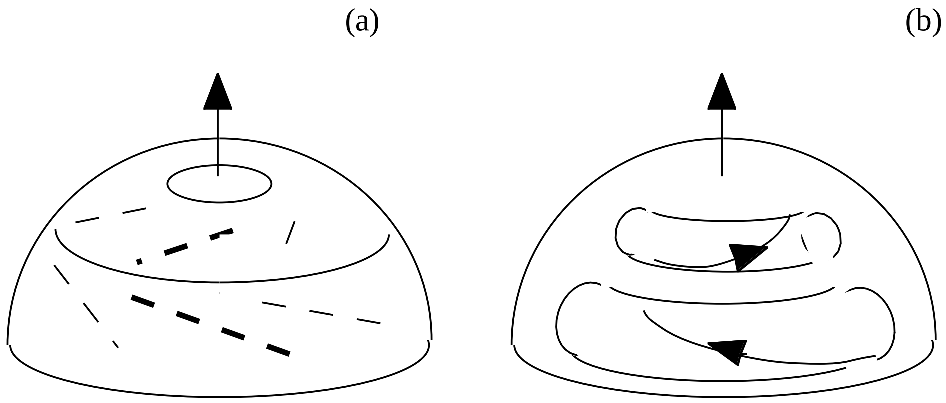

Fig.5 Observed magnetic field direction on the surface of northern hemisphere is shown by dotted lines in (a). A pair of tori with opposite helicity in the northern hemisphere.

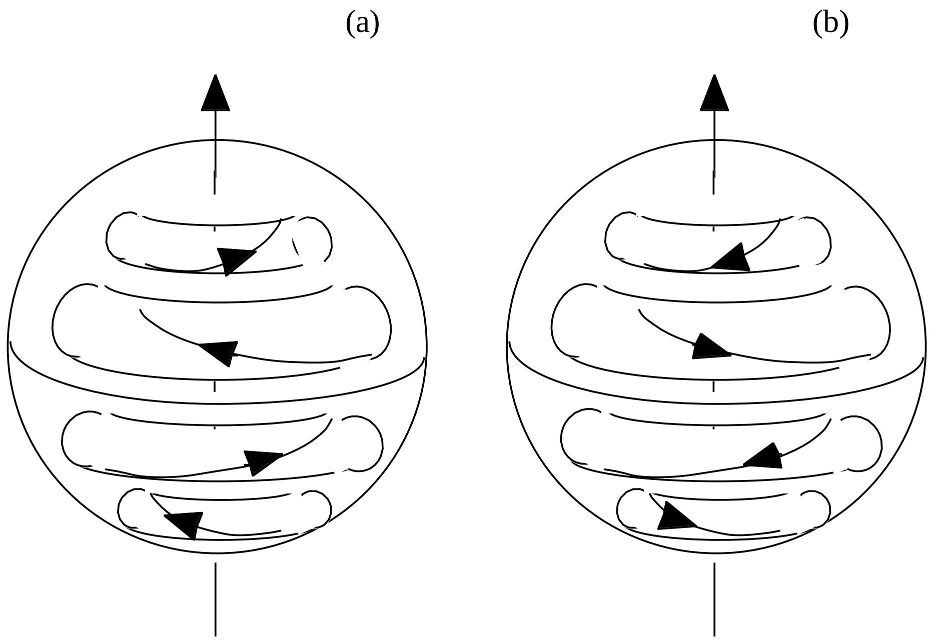

Fig.6 Schematic drawing of the toroidal magnetic field. (a9 and (b) illustrates the two phases of opposite sign of magnetic field.

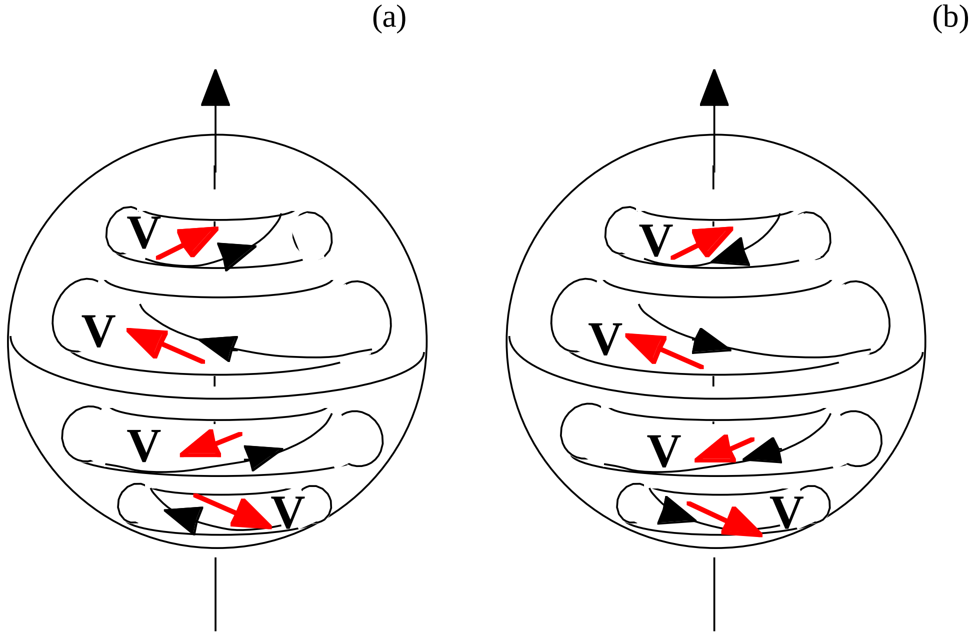

Fig.7 Schematic drawing of the toroidal magnetic and flow structures. Black arrow indicates the magnetic field and the red arrows indicate the flow velocity. The case of the sign of the magnetic field in the case of Fig.3 is shown in (a). (b) shows the case when the sign of the magnetic field is reversed, owing to the solar magnetic cycle. In both cases, the poloidal flow which is driven by the cross-helicity dynamo is pole-ward.